

22 **Abstract**

23 Iron plays vital roles in important biological processes in fish, but can be toxic in high
24 concentrations. The information on metalloproteins that participate in maintenance of Fe-
25 homeostasis in an esocid fish, the northern pike, as an important freshwater bioindicator
26 species, are rather scarce. The aim of this study was to identify main cytosolic constituents that
27 sequester Fe in the northern pike liver. The method applied consisted of two-dimensional
28 HPLC separation of Fe-binding biomolecules, based on anion-exchange followed by size-
29 exclusion fractionation. Apparent molecular masses of two main Fe-metalloproteins isolated by
30 this procedure were ~360 kDa and ~50 kDa, with the former having more acidic pI, and
31 indicated presence of ferritin and haemoglobin, respectively. MALDI-TOF-MS provided
32 confirmation of ferritin subunit with a m/z peak at 20.65 kDa, and haemoglobin with spectra
33 containing main m/z peak at 16.1 kDa, and smaller peaks at 32.1, 48.2, and 7.95 kDa (single-
34 charged Hb-monomer, dimer, and trimer, and double-charged monomer, respectively). LC-
35 MS/MS with subsequent MASCOT database search, confirmed the presence of Hb- β subunits
36 and pointed to close relation between esocid and salmonid fishes. Further efforts should be
37 directed towards optimization of the conditions for metalloprotein analysis by mass
38 spectrometry, to extend the knowledge on intracellular metal-handling mechanisms.

39

40 **Key words:** ferritin, fish, haemoglobin, HPLC, liver, MALDI-TOF-MS

41

42 **1. Introduction**

43

44 Iron is an essential trace element for fish and other living organisms, vital for important
45 biological processes (e.g., oxygen and electron transport, cellular respiration, synthesis of DNA
46 and neurotransmitters) [1-3]. Biological activity of Fe, as of many other trace elements, is
47 primarily associated with their binding to various proteins, thus forming metalloproteins, in
48 which metals are essential components [2]. Iron deficiency can cause a number of disorders of
49 different degrees of severity [2]. However, in excess, even essential trace metal like Fe can be
50 toxic, causing the reactive oxygen species formation, and consequently leading to lipid
51 peroxidation, DNA damage, altered calcium homeostasis, and eventually cell death [2-5].
52 Since there is a fine line between metal essentiality and toxicity, organisms have developed
53 complex systems for maintenance of trace element homeostasis, which are composed chiefly of
54 transport and storage proteins, and certain hormones [2]. Following the uptake in the organism,
55 Fe is transported in a bloodstream as a complex with transferrin, being finally delivered to cells
56 of target organs. In the cytoplasm of those cells, Fe is present within the labile Fe-pool, whereas
57 excess Fe is stored in ferritin [2,3].
58 Ferritins play a key role in Fe metabolism by sequestering potentially toxic free Fe, and
59 maintaining Fe in a soluble, nontoxic, bioavailable form [6,7]. Ferritin has a mass of ~450 kDa,
60 and consists of a central hydrous ferric-oxide phosphate core surrounded by an outer protective
61 hollow protein shell called apoferritin [3,6]. The apoferritin has 24 subunits (a combination of
62 heavy (H) and light (L) chains; molecular masses in a range from 18 to 28 kDa) [6-8]. The H-
63 chains are associated with active role in Fe metabolism, including ferroxidase activity, whereas
64 L-chains are associated with a long-term storage function [7-9]. Thus, ferritins rich with L-
65 chains are typical for organs with high Fe storage, such as the liver [3]. However, the native
66 ferritins from different fish livers contain only one (middle) type of subunit instead of two,
67 which possesses the characteristics of both H and L subunits [3,6,7] (in liver of smooth

68 hammerhead (*Sphyrna zygaena*), 21 kDa [7]; in liver of the northern pike (*Esox lucius*), 20.4
69 kDa [10]).

70 Moreover, haemoglobin (Hb), which is contained in erythrocytes, contains Fe which reversibly
71 binds oxygen and functions as the final acceptor of electrons originating from oxidative
72 catabolic reactions [11-13]. The Hb molecule in vertebrates contains four globin chains (two α
73 and two β) in a stable tetramer, each of them containing a prosthetic heme group which
74 participates in oxygen binding through an iron atom in the ferrous form (Fe^{2+}) [13]. Heme
75 group is apparently identical in every studied fish species, whereas the globins differ from
76 species to species and among Hb isoforms [12,13]. The great majority of fish species have
77 symmetric Hbs, i.e., two pairs of identical globin chains [13]. In the studies of fish liver
78 metalloproteins, it is expected to detect Hb, as liver is perfused by blood [14].

79 Iron metalloproteins in freshwater fish were studied in various species (e.g., belonging to
80 families Channidae, Cyprinidae, Esocidae, Leuciscidae, Salmonidae) by many different
81 methods (e.g., PCR analysis and immunohistochemistry, electrophoresis, various
82 immunological, chromatography and mass spectrometry methods), with the special emphasis
83 on Hb and ferritin studies [3,6,10,14-19].

84 The studies on Fe-metalloproteins in the northern pike are fairly scarce. In addition to our studies
85 on hepatic Fe-metalloproteins, by one-dimensional size exclusion or ion exchange
86 chromatography coupled with inductively coupled plasma mass spectrometry (ICP-MS)
87 [18,19], only study that we are aware of is the one on hepatic ferritin as a possible natural iron
88 supplement [10].

89 The current study aims to supplement our two previous studies [18,19] by identification of the
90 main Fe-binding biomolecules in the northern pike liver using two-dimensional
91 chromatographic separation and subsequent mass spectrometry detection. Additional aim is to
92 associate our results with those contained in databases (applying MASCOT search), and
93 compare it subsequently with our corresponding study on the Vardar chub (*Squalius*

94 *vardarensis*) [14], to establish relationships among various fish species with the regard to
95 intracellular Fe-handling strategies.

96

97 **2. Materials and methods**

98

99 *2.1. Fish sampling and the dissection of liver*

100 The sampling of the northern pike (*E. lucius* Linnaeus, 1758) was carried out on 22nd April and
101 1st May 2021 from the Mrežnica River (Croatia) in front of the former cotton industry facility in
102 Duga Resa town (N 45° 27' 4,38" E 15° 30' 18,96") using an electrofishing device (Hans Grassl,
103 EL63 II GI, 5.0 KW, 137 Honda GX270, 300/600V max., 27/15A max.), in accordance with
104 the Croatian standard HRN EN 14011 [20]. Following the requirements of the Ordinance on the
105 protection of animals used for scientific purposes [21], the fish were euthanized at the location
106 of the sampling, immediately after being caught, using unbuffered MS 222 (tricaine methane
107 sulphonate, Sigma Aldrich) in concentration of ~50 mg L⁻¹ and in duration under 10 min [17].
108 Fish length and mass were measured, age was determined by counting the number of annuli
109 (rings) on scales using Olympus BH2 microscope (magnification 30×), whereas sex was
110 determined by gonad examination at macroscopic level. The liver were taken from each fish
111 and then stored, first in the liquid nitrogen and thereafter in the freezer at -80°C, until further
112 processing. Seventeen fish were caught in total at this location at the said dates, and liver of
113 three of them were selected for this particular investigation (the same three northern pike
114 specimens as used and presented in our previous paper) [19]. Three studied northern pike
115 specimens were of the following characteristics: total mass of 345–1100 g; total length of 36.5–
116 54.0 cm; they were all female with the age span from 2+ to 4+.

117

118 *2.2. Homogenization and centrifugation of the northern pike liver*

119 The liver were cut to pieces in glass containers placed on ice, and then into each container we
120 have added cold homogenization buffer [100 mM Tris-HCl/Base (Sigma Aldrich, USA; pH 7.5

121 at 4 °C) supplemented with reducing agent (1 mM dithiothreitol (DTT), Sigma Aldrich, USA)]
122 (ratio of m_{liver} and v_{buffer} was 1+5). Hepatic tissue suspensions were homogenized in an ice-
123 cooled tube by 10 strokes of Potter-Elvehjem homogenizer (Glas-Col, USA) at 6000 rpm. The
124 homogenates were thereafter centrifuged for 2 h at 50,000×g and +4 °C (Avanti J-E centrifuge,
125 Beckman Coulter, USA). The resulting supernatants (S50) represented soluble hepatic
126 fractions, which mainly refer to cytosol, and further contain only microsomes [22] and
127 extracellular fluids (including traces of blood). Thus obtained hepatic cytosols were
128 immediately stored at -80 °C, and kept there until further analyses [18].

129

130 *2.3. High resolution (HR) ICP-MS measurement of Fe and other element concentrations in the* 131 *northern pike hepatic cytosols*

132 The volumes of 300 µL of hepatic cytosols were first digested using the digestion mixture
133 containing nitric acid (HNO₃; *Normatom*® 67–69 % for trace element analysis, VWR
134 Chemicals, UK) and hydrogen peroxide (H₂O₂; *Suprapur*® 30 %, Merck, Germany) in volume
135 ratio 3+1. Volume ratio of cytosol to digestion mixture was 1+1. For each of the three samples,
136 the digestion was carried out in duplicate in the laboratory dry oven (at 85 °C; 3.5 h) [18]. In
137 thus obtained digested samples, diluted five times with Milli-Q water, Fe concentrations were
138 measured using HR ICP-MS (Element 2, Thermo Finnigan, Germany). Measurements of ⁸²Se,
139 ⁹⁵Mo, ¹⁰⁹Ag, ¹¹¹Cd, ¹³³Cs, ²⁰⁵Tl, ²⁰⁸Pb, and ²⁰⁹Bi were performed in low resolution mode, of
140 ⁵⁵Mn, ⁵⁶Fe, ⁵⁹Co, ⁶³Cu, and ⁶⁶Zn in medium resolution mode, and of ⁷⁵As in high resolution
141 mode. External calibrations were applied, which were based on adequate dilutions of
142 multielement standard solution for trace elements (Analytika, Czech Republic) prepared in 2 %
143 (vol.) HNO₃ (*Normatom*® 67-69 % for trace element analysis, VWR Chemicals, UK)
144 supplemented with adequately diluted standard solutions of Cs (1 g L⁻¹; Fluka, Germany). The
145 elemental concentrations used for creation of calibration curves were 0, 1, and 10 µg L⁻¹ for all
146 studied elements, and additionally 100 µg L⁻¹ for Cu, 500 µg L⁻¹ for Cu, Fe, and Zn, and 1000
147 µg L⁻¹ for Fe and Zn, with respect to their actual concentrations in the analysed samples. To all

148 the samples and calibration standards, In (Fluka, Germany) was added as an internal standard (1
149 $\mu\text{g L}^{-1}$). The cytosolic concentrations of all 14 analysed elements in the northern pike liver are
150 presented in Table 1, and, additionally, Fe concentrations in the selected northern pike hepatic
151 cytosols are presented in Fig. 1.

152 Limits of detection (LOD) for HR ICP-MS measurement of Fe and other studied elements in
153 digested and diluted hepatic cytosols were calculated based on the three standard deviations of
154 ten successively measured metal/metalloid concentrations in the blank sample (comprised of
155 homogenization buffer, HNO_3 and H_2O_2 , and processed using the same procedure as used for
156 the digestion of hepatic cytosols). The obtained LODs (ng of element per g of hepatic tissue)
157 were the following: Ag, 0.37; As, 1.40; Bi, 0.24; Cd, 0.08; Co, 0.22; Cs, 0.10; Cu, 16.3; Fe, 75;
158 Mn, 1.7; Mo, 0.21; Pb, 0.49; Se, 1.5; Tl, 0.001; and Zn, 23. The HR ICP-MS measurement of
159 several elements with certified concentrations in quality control sample (UNEP GEMS,
160 Canada) on two separate occasions resulted with the following recoveries (average \pm standard
161 deviation): As, 100.7 ± 0.6 %; Cd, 102.6 ± 1.1 %; Co, 101.9 ± 5.6 %; Cu, 102.2 ± 0.5 %; Fe,
162 95.8 ± 0.1 %; Mn, 103.0 ± 1.0 %; Mo, 101.6 ± 2.5 %; Pb, 99.4 ± 1.5 %; and Zn, 107.1 ± 2.4 %.

163

164 *2.4. Two-dimensional high performance liquid chromatography (HPLC) separations of Fe-* 165 *binding biomolecules from the northern pike hepatic cytosol*

166 During all chromatographic separations, we have undertaken all the necessary measures, as
167 mentioned by de la Calle Guntiñas et al. [23], which are required to avoid metal dissociation
168 from metal-binding biomolecules and maintain the physiological surroundings, such as the use
169 of ice-cold conditions during the sample handling, and the constant pH of 7.4 throughout the
170 HPLC-separations.

171

172 *2.4.1. Anion exchange (AEX)-HPLC-ICP-MS analysis*

173 The first step of separation of Fe-binding biomolecules from the northern pike hepatic cytosol,
174 with subsequent Fe detection, was based on AEX-principle (i.e., separation based on

175 differences in net charges) using hyphenated HPLC-ICP-MS system (HPLC, Agilent 1260
176 Infinity II with a diode array UV/VIS detector; ICP-MS, Agilent 7900; Agilent Technologies,
177 USA). The analyzed sample was the soluble hepatic fraction of the northern pike. The protocol
178 for AEX-HPLC separation was described in our previous paper [19], and adapted from the
179 previously described procedures [14,24]. The details on separation protocol are given in Table
180 2. In Fig. 1 we have presented only the obtained AEX-HPLC-profiles for Fe, since the
181 comparison with several other metals was already discussed in details in our previous paper
182 [19]. Selected Fe-containing AEX-fractions were collected in plastic tubes at 30 sec intervals
183 using a fraction collector (Agilent InfinityLab LC Series 1260 Infinity II Bio-inert Fraction
184 Collector). Fractions were supplemented with 1 mM DTT (Honeywell Fluka, Germany) and
185 then pooled under ice-cold conditions and preconcentrated by Amicon Ultra centrifugal filters
186 (cut off at 3kDa, Merck, Millipore, Ireland) for second step of chromatographic separation. Iron
187 recovery from AEX-column was calculated to be 85–97%, based on the analyses of samples 1
188 and 2. During recovery estimation, quality control indicated measurement accuracy in the range
189 from 99–104%.

190

191 2.4.2. Size exclusion (SEC₂₀₀)-HPLC-ICP-MS analysis

192 The second step of chromatographic separation was based on size exclusion principle (i.e.,
193 separation based on differences in molecular masses), using the same hyphenated HPLC-ICP-
194 MS system as described above. The details on separation protocol are given in Table 2. In order
195 to identify potential overlapping peaks of the other metals/metalloids with Fe-peaks, in addition
196 to Fe we have also measured 13 other elements (Ag, As, Bi, Cd, Co, Cs, Cu, Mn, Mo, Pb, Se,
197 Tl, and Zn) in selected AEX-fractions separated by SEC₂₀₀-column. The results are presented in
198 Fig. 2-4 and Table ESM.1 (see Electronic Supplementary Material). For the column calibration,
199 six protein standards were run through the column under the same conditions as the samples
200 and their elution times, void volume elution time, and calibration straight line equation are
201 shown in Table 3. Metal-binding biomolecules were defined as belonging to the high molecular

202 mass region (HMM, >100 kDa), the medium molecular mass region (MMM, 30–100 kDa), and
203 the low molecular mass region (LMM, <30 kDa).

204 Selected SEC₂₀₀-fractions were collected in plastic tubes at one minute intervals, supplemented
205 with 1 mM DTT (Honeywell Fluka, Germany), pooled under ice-cold conditions and
206 pre-concentrated by Amicon Ultra centrifugal filters (cut off at 3kDa, Merck, Millipore, Ireland)
207 for further mass spectrometry analysis.

208

209 *2.5. Mass spectrometry analysis of selected AEX-SEC₂₀₀-HPLC-fractions of the northern pike*
210 *hepatic cytosol*

211 After two-dimensional chromatographic fractionation (AEX-SEC₂₀₀-HPLC), selected Fe-
212 containing fractions were further analyzed with two mass spectrometry techniques (MALDI-
213 TOF-MS (matrix-assisted laser desorption/ionization time of flight mass spectrometry) and LC-
214 MS/MS (liquid chromatography tandem mass spectrometry)) in order to determine exact
215 molecular masses and possibly identify the isolated northern pike hepatic biomolecules of
216 interest.

217

218 *2.5.1. MALDI-TOF-MS analysis*

219 For the purpose of MALDI-TOF-MS analysis, we have used bench-top Bruker Microflex LT
220 mass spectrometer equipped with the Bruker flexControl v 3.4 and flexAnalysis v 3.4 software
221 (Bruker Daltonics, Germany). The volumes of 1 µL of pre-concentrated samples were spotted in
222 two replicates onto a 96-spot steel target plate (Bruker Daltonik, Germany) and allowed to
223 visibly dry at room temperature. Subsequently, 1 µL of HCCA matrix, containing α -cyano-4-
224 hydroxycinnamic acid (10 mg mL⁻¹; Bruker Daltonik, Germany) in 50% acetonitrile (Optima®
225 LC/MS grade, Thermo Fisher Scientific, UK) and 2.5% trifluoroacetic acid (Sigma Aldrich,
226 USA), was added on top of the samples and allowed to dry at room temperature.

227 Modified protocol by Huang et al. [7] was used to analyze fractions containing HMM Fe-
228 binding biomolecules. Volumes of 5 µL of samples were mixed with 5 µL of acetone (Thermo

229 Fisher Scientific, UK) and 5 μL of the HCCA matrix. Volume of 5 μl of the this mixed solution
230 was loaded onto the target plate, and the solvent was removed by air drying.

231 The mass spectra were acquired manually. Ions were captured in the positive linear mode (mass
232 range 5-100 kDa), and positive ions were extracted at accelerated voltage of 20 kV. Spectra
233 with the sum of the ions were obtained by 1000 laser shots in different regions of every target
234 plate spot. The results are presented in Fig. 5.

235

236 *2.5.2. LC-MS/MS analysis with MASCOT database search*

237 LC-MS/MS analyses with MASCOT database search were performed in accordance with the
238 method described in our previously published paper [14], which will be presented further on in
239 detail. In preconcentrated AEX-SEC₂₀₀-fractions, DTT (Honeywell Fluka, Germany) was again
240 added in a concentration of 1 mM in order to reduce possible disulfide bonds in the proteins.

241 After 1 hour at room temperature, 54 mM iodoacetamide (Sigma Aldrich, USA) was added to
242 the reaction mixture to a final concentration of 5.5 mM and left in the dark at room
243 temperature for another hour. Finally, 1 μL of trypsin (1 $\mu\text{g } \mu\text{L}^{-1}$; Trypsin Gold, Promega,
244 USA) was added and the mixture was incubated overnight at room temperature. The reaction
245 was stopped by adding trifluoroacetic acid (Sigma Aldrich, USA) to a final concentration of
246 1%.

247 Analyses of obtained samples of tryptic peptides were performed via low resolution ion trap
248 LC-MS/MS (LC, Dionex Ultimate 3000 RSLC; MS/MS, Amazon ETD ion trap; Bruker
249 Daltonik, Germany). Peptides were loaded onto a trap column (C18 resin, Acclaim Pepmap,
250 100 \AA , 5 mm, 1 mm, 5 mm) in 1 mL of solution containing 0.1% formic acid (Fisher Chemical,
251 UK). Peptides were separated on a capillary column (C18 resin, Acclaim Pepmap, 100 \AA , 2
252 μm , 0.3 mm x 150 mm) at a flow rate of 3.5 $\mu\text{L min}^{-1}$. Mobile phase A consisted of 0.1%
253 formic acid in solution of HPLC grade water (98%) /acetonitrile (2%), and mobile phase B
254 consisted of 0.1% formic acid in solution of acetonitrile (98%) / HPLC grade water solution
255 (2%). The 45 min multistep gradient consisted of mobile phase B: 1 min 5%, 30 min linear

256 gradient to 45%, 1 min linear gradient to 90%, 4 min hold on 90%, 3 min linear gradient to 5%,
257 6 min hold on 5%. The MS/MS was operated at an ESI capillary voltage of 4500 V. High
258 voltage end plate offset was 500 V. The nebulizer was set at 10 psi.
259 The temperature of dry gas was set at 300 °C with a flow rate of 8 L min⁻¹. Helium was used as
260 a collision gas. The fragmentation amplitude was set at 0.60 V and ramped between 30% and
261 300% of this value. Product ion spectra were sequentially recorded for each selected precursor.
262 The acquisition software was set up in autoMS/MS mode using up to three precursor ions with
263 enabled active exclusion (precursor exclusion after two MS/MS spectra for 2 min). MS and
264 MS/MS spectra were acquired within a scan range from 300 to 1500 *m/z* using averages from
265 five spectra and a scan rate of 8100 (*m/z*) s⁻¹. DataAnalysis software 4.0 (Bruker Daltonik
266 GmbH, Germany) was used to extract MS and MS/MS data to create a Mascot file for database
267 search.
268 Search parameters were enzyme trypsin cleavage, allowed two missed cleavages, fixed
269 modification carbamidomethyl and variable modification methionine oxidation, mass tolerance
270 0.5 Da. The NCBI non-redundant database version 18122019 and UniProt/Swiss-Prot
271 sprot_15042019 was used as a protein sequence database. The results are presented in Tables 4
272 and 5, and in Electronic Supplementary Material.

273

274 *2.6. Data processing and graphical data presentation*

275 All calculations (e.g., SEC-HPLC calibration, calculations of molecular masses associated to
276 individual metal SEC-HPLC peaks) were executed in Microsoft Office Excel (version 16). The
277 graphs were created in statistical program SigmaPlot 11.0 for Windows.

278

279 **3. Results and discussion**

280 We have started our study on metalloproteins/peptides in the liver of the northern pike
281 (including Fe-binding biomolecules) by establishing the distributions of several elements of
282 interest among the biomolecules of different sizes (by use of SEC-HPLC; Dragun et al., 2022)

283 and their distribution among the biomolecules of different total charges (by use of AEX- and
284 CEX-HPLC) [19].

285 Our previously published one-dimensional chromatographic separation of the northern
286 pike hepatic cytosol applying the SEC₂₀₀-column [18] revealed predominant Fe binding to
287 HMM biomolecules. Major obtained Fe-peak in that study had HPLC-estimated molecular
288 mass maximum at ~400 kDa (range ~200-600 kDa), near the elution time of standard protein
289 apoferritin (molecular mass 443 kDa), leading to a conclusion that it referred to Fe-storage
290 protein ferritin [18]. Another prominent Fe-peak reported in that study was obtained with
291 maximum at ~50 kDa (range ~30-80 kDa; Fe-MMM-peak), and based on the comparison with
292 the previously published reports [14-17,25], it was hypothesized to be Hb [18]. We have also
293 reported that increase in Fe bioaccumulation in liver of the northern pike resulted with the
294 increased quantity of Fe associated with the SEC₂₀₀-HMM-peak, i.e. presumably ferritin [18].

295 Moreover, our previously published one-dimensional chromatographic separation of
296 the northern pike hepatic cytosol applying the AEX/CEX-columns [19] revealed that more than
297 95% of Fe-metalloproteins binds to the AEX-column at physiological pH (7.4), i.e. has
298 negative total charge and acidic isoelectric point. Moreover, in that study, Fe was found in five
299 peaks eluted from the AEX-column (Fig. 1) [19]: the first two were poorly resolved (max. at E_t
300 of 9.1 and 9.3 min) and, compared to standard proteins, had pIs close to neutral values, whereas
301 the majority of eluted Fe was associated with the third AEX-peak (max. at E_t of 10.6 min)
302 which, compared to standard proteins, had pI probably within pH range of 4-6; the remaining
303 two Fe-peaks were observed with maxima at E_t of 14.7 and 18.8 min, indicating more acidic
304 Fe-binding biomolecules. Based on the comparison with our previously published SEC₂₀₀-
305 analysis [18], we have presumed that the major Fe-AEX-peak referred to ferritin, whereas the
306 first two peaks (containing second highest Fe-quantity) possibly referred to Hb. The plausibility
307 of that conclusion was further corroborated by the known pIs of these two Fe-metalloproteins
308 (pI_{ferritin} in fish liver: 4.1-7.0 [6]; pI_{Hb} in fish liver: 5.9-8.1 [26]) (see Electronic Supplementary
309 Material, Table ESM.2). We have also reported that increase in Fe bioaccumulation in liver of

310 the northern pike resulted with the increased quantity of Fe associated with the probable AEX-
311 ferritin peak [19].

312 However, to be able to associate undoubtedly the Fe-SEC₂₀₀-peaks of particular
313 molecular masses with specific Fe-AEX-peaks, i.e. to define the relations between the main Fe-
314 binding biomolecules regarding their molecular masses and total charges, two-dimensional
315 chromatographic separation had to be performed, with either additional AEX-HPLC separation
316 of chosen SEC₂₀₀-peaks, or additional SEC₂₀₀-HPLC separation of chosen AEX-peaks. Two-
317 dimensional HPLC-fractionation is further beneficial because it enables the purification of the
318 biomolecules of interest and their more reliable identification by further analysis using mass
319 spectrometry methods [14]. Namely, when SEC₂₀₀-HPLC fractionation was applied, coelution
320 of Fe with several other elements was observed (Bi, Co, Mn, Mo, and Zn coeluted with HMM-
321 Fe-peak; Bi, Co, Cu, Mn, Se, and Zn coeluted with MMM-Fe-peak) indicating that each
322 SEC₂₀₀-peak contains a mixture of metalloproteins [18]. The same conclusion could be made
323 for fractionation by AEX-column, where Fe-binding biomolecules were eluted together with
324 biomolecules that bind Ag, Bi, Cd, Co, Cu, Mn, Pb, Tl, and Zn [19].

325 Thus, as a starting point in this study, we have chosen Fe-AEX-profile (Fig. 1), and for
326 further SEC₂₀₀-HPLC separation collected the AEX-fractions containing the first three major
327 Fe-AEX-peaks (eluted from 8.5 to 11.5 min). Since the peaks are placed rather close to one
328 another, and it is difficult to separate them clearly due to a possibility of minor variability of
329 elution time between chromatographic runs, we have collected and pooled four fractions, as
330 follows: AEX-fraction A, 8.5-9.5 min; AEX-fraction B, 9.5-10.0 min; AEX-fraction C, 10.0-
331 10.5 min; and AEX-fraction D, 10.5-11.5 min.

332

333 *3.2. SEC₂₀₀-HPLC-ICP-MS analysis of Fe in selected AEX-HPLC fractions, as a second* 334 *dimension of fractionation of Fe-binding biomolecules*

335 The Fe-profiles obtained by SEC₂₀₀-HPLC-ICP-MS for four above mentioned AEX-
336 fractions are presented in the Fig. 2. As said above, the tails of AEX-Fe-peaks overlapped to a

337 certain degree, and thus in each fraction it was possible to observe appearance of one Fe-peak
338 and/or disappearance of another. Accordingly, it can be observed that Fe-binding biomolecule
339 of molecular mass of ~50 kDa appears already in the earliest AEX-fraction (A: 8.5-9.5 min;
340 Fig. 2a), and has its maximum in the second one (B: 9.5-10.0 min; Fig. 2b), and then gradually
341 disappears (Figs. 2c,d). On the other hand, Fe-binding biomolecule of molecular mass of ~360
342 kDa appears already in the second AEX-fraction (B: 9.5-10.0 min; Fig. 2b), but has its
343 maximum in the last two fractions (C and D: 10.0-11.5 min; Fig. 2c,d). The results obtained by
344 two-dimensional chromatographic separation have thus confirmed our hypothesis on the
345 association between the Fe-SEC₂₀₀-peaks of particular molecular masses with specific Fe-AEX-
346 peaks. It was confirmed that presumable ferritin peak of higher molecular mass has earlier
347 SEC₂₀₀-elution time and later AEX-elution time (more acidic pI) compared to the other major
348 Fe-binding biomolecule, presumably Hb, of lower molecular mass, i.e. later SEC₂₀₀-elution
349 time, and earlier AEX-elution time (pI closer to neutral values).

350 Since our aim was also to purify Fe-binding biomolecules, to be able to identify them
351 more reliably, in addition to Fe we have measured 13 other elements in AEX-fractions
352 separated by SEC₂₀₀-column, and their peak maxima are presented in Table ESM.1 (see
353 Electronic Supplementary Material). It can be seen that the majority of metals/metalloids were
354 separated from Fe, and overlapping peaks with 50 kDa Fe-peak were found only for Mn, Pb,
355 and Se (see Electronic Supplementary Material, Table ESM.1; Fig. 3), and with 360 kDa Fe-
356 peak for Pb and Zn (see Electronic Supplementary Material, Table ESM.1; Fig. 4). This,
357 however, had to be considered during the interpretation of mass spectrometry analysis, for
358 which we have chosen the fractions marked in the Fig. 2b (~50 kDa; collected from 23 to 26
359 min) and Fig. 2c (~360 kDa; collected from 17 to 19 min).

360

361 *3.3. MALDI-TOF-MS analysis of selected AEX-SEC₂₀₀-HPLC fractions*

362 The analysis of 360 kDa Fe-peak resulted with a MALDI-peak at m/z equal to 20.65
363 kDa (Fig. 5a). This finding closely corresponds to molecular mass of ferritin subunits

364 previously reported for the northern pike liver (20.4 kDa) [10], thus indicating that the detected
365 peak refers to single charged ferritin subunit. Similar molecular mass was reported for the liver
366 of *S. zygaena* (~21 kDa) [7]. The finding of subunits instead of the intact ferritin molecule is
367 very common since, as explained by Huang et al. [7], even high laser intensity in MALDI-TOF
368 MS does not have capacity to make a molecular ion of a whole protein for mass determination
369 of ferritin, because its molecular mass is too big (>400 kDa). However, high laser intensity can
370 weaken binding energy of noncovalent bonds among ferritin subunits, creating their molecular
371 ions detectable by mass spectrometry [7]. Huang et al. [7] managed to detect single charged
372 ferritin subunit of 21.07 kDa in the liver of *S. zygaena*, together with double charged
373 monomers, and single charged dimers and trimers, but only after they applied high laser
374 intensity, whereas application of low laser intensity did not produce visible spectra. In our
375 study, even laser intensity of 90%, resulted with an m/z -peak characteristic for ferritin subunit
376 in only one sample and having very low intensity (~100; Fig. 5a), indicating the possibility that
377 the bonds among ferritin subunits in liver of the northern pike, without any pretreatment, were
378 too strong for the potential of the applied instrument. However, there is another possible
379 explanation for absence/low intensity of MALDI-peak of ferritin in the collected HMM-
380 fraction of the northern pike liver. There is a possibility that the concentration of this Fe-
381 binding biomolecule was too low in our collected HPLC-fractions. Although the intensity of Fe
382 in this HMM-peak was high (Fig. 2), it has to be taken in consideration that one molecule of
383 ferritin can store up to 4500 Fe^{3+} ions [27,28], and thus high intensity of Fe does not necessarily
384 reveal high protein concentration. Accordingly, our further research will be focused on the
385 optimization of the pretreatment and conditions for mass spectrometry analysis of Fe-binding
386 proteins of high molecular masses.

387 The analysis of 50 kDa Fe-peak obtained from two fish samples resulted with a
388 detectable MALDI-spectra (Fig. 5b), containing several m/z peaks. The main peak was
389 observed at 16.05 kDa, presumably indicating single-charged Hb-subunit, which is typical
390 MALDI-spectra for Hb according to available literature [14,29,30]. For example, in hemocytes

391 of whiteleg shrimp *Litopenaeus vannamei*, Hb was detected as a subunit (Hb β) of 16.12 kDa
392 [29], and in the liver of Vardar chub (*S. vardarensis*) as a subunit (Hb β) of 15.4 kDa [14]. It is
393 not unusual to detect subunits by MALDI-TOF MS instead of intact protein, because, as
394 mentioned above, the laser in this method can decompose unstable multisubunit proteins into
395 the free subunits [7]. In addition, we have observed much smaller peaks at 32.12 kDa and 48.19
396 kDa, as a possible sign of presence of dimers and trimers of Hb-subunits, whereas tetramer (i.e.
397 intact protein) was not detected. Similar finding was reported for Vardar chub liver, with
398 detected dimers (31.5 kDa) and trimers (46.9 kDa) [14]. A peak recorded at 7.95 kDa possibly
399 indicated double-charged Hb-subunit (Fig. 5b). The same was also reported for human blood,
400 where Hb was detected by MALDI-TOF-MS as a double charged subunit (Hb α -chain) with
401 m/z equal to 7.56 kDa [30]. In the MALDI-TOF-MS spectra, several other small peaks were
402 observed, which can be explained by the fact that the isolated protein was not completely
403 purified, but contained the traces of metalloproteins that bind Mn, Pb, and/or Se (see Electronic
404 Supplementary Material, Table ESM.1, Fig. 3).

405

406 *3.4 LC-MS/MS analysis of selected AEX-SEC₂₀₀-HPLC fraction with subsequent MASCOT* 407 *search*

408 Finally, only Fe-binding protein of HPLC-estimated molecular mass equal to ~50 kDa
409 (AEX-E_t: 9.5-10.0 min, SEC₂₀₀-E_t: 23-26 min;), that was isolated from the liver of the northern
410 pike from the Mrežnica River, was detected by LC-MS/MS analysis. Subsequent MASCOT
411 search of two databases (UniProt/Swiss-Prot, NCBIInr) recognized it as Hb-subunit β (Hb β),
412 based on the similarities with Hb β sequences stored in the databases for northern pike and
413 sockeye salmon (*Oncorhynchus nerka*) (Table 4). Our previous LC-MS/MS study combined
414 with MASCOT search of corresponding Fe-binding protein from the liver of Vardar chub also
415 indicated the presence of Hb β subunits, but the similarities were obtained with Hb β sequences
416 stored in the databases for fishes *Danio rerio*, *Carassius auratus*, and *Arctogadus glacialis*
417 [14].

418 Among the different fish species, the high degree of genetic variation was detected
419 [13,31]. Thus, the studies of metal-binding biomolecules conducted on various species enable
420 the identification of similarities/differences in metal handling strategies among different fish
421 species, families, and/or orders. Based on our two so far performed studies of this kind, we
422 have identified the following grouping regarding the Fe-sequestering by Hb within the class
423 Teleostei (teleosts) (Table 4; [14]): (1) [Esociformes (order, pikes and mudminnows) >
424 Esocidae (family, pikes) > *Esox lucius* Linnaeus, 1758 (species, the northern pike)] was
425 associated with [Salmoniformes (order, salmon) > Salmonidae (family, salmon) >
426 *Oncorhynchus nerka* (Walbaum, 1792) (species, the sockeye salmon)]; (2) [Cypriniformes
427 (order, carps) > Leuciscidae (family, minnows) > *Squalius vardarensis* Karaman, 1928
428 (species, the Vardar chub)] was associated with [Cypriniformes (order, carps) > Danionidae
429 (family, danios) > *Danio rerio* (Hamilton, 1822) (species, the zebrafish)], [Cypriniformes
430 (order, carps) > Cyprinidae (family, minnows or carps) > *Carassius auratus* (Linnaeus, 1758)
431 (species, the goldfish)], and [Gadiformes (order, cods) > Gadidae (family, cods and haddock)
432 > *Arctogadus glacialis* (Peters, 1872) (species, the Arctic cod)]. Similarity in metal-handling
433 strategy between esocids and salmonids, and between leuciscid and cyprinid fish, were already
434 observed when Zn distribution among cytosolic biomolecules was studied using SEC-HPLC-
435 ICP-MS [18].

436 Furthermore, MASCOT search resulted with several additional hits (Table 5). Some of
437 them were immediately dismissed as improbable (DNA-directed RNA polymerase subunit β ,
438 caskin-2, pre-mRNA-splicing factor prp12, genome polyprotein, tRNA (Met) cytidine
439 acetyltransferase; Table 5) due to much higher mass of the intact protein or a subunit
440 (molecular mass: ~120-330 kDa; Table 5) compared to molecular mass estimated by SEC₂₀₀-
441 HPLC (~30-80 kDa; Fig. 2). In some cases, an additional reason for dismissal was protein
442 intracellular location (e.g., nuclear placement of prp12 [32]) or species of origin (genome
443 polyprotein inherent to viruses [33]). Five MASCOT hits seemed plausible according to
444 molecular masses (18–46 kDa), however some other features rendered most of them unlikely.

445 Since we have isolated soluble, cytosolic, hepatic fraction, containing additionally only
446 microsomes [22], we have concluded that most likely the proteins characteristic for organelles
447 and membrane were not contained within the studied fraction. Those included ribosomal
448 proteins (ribosomal RNA large subunit methyltransferase, 30S ribosomal protein S3; Table 5)
449 and transmembrane transporter (ATP-binding cassette domain-containing protein [34]). Which
450 left us with only two additional options, i.e. two enzymes of acceptable molecular mass
451 (fumarylacetoacetase (FAH), 46.5 kDa; and malate dehydrogenase (MDH), 38.4 kDa; Table 5),
452 which have pI close to neutral pH values, and cytoplasmic placement in the cell (according to
453 Malécot et al. [35] and Table 5, respectively). According to literature reports, FAH is cytosolic
454 homodimer with two 46 kDa subunits, where equilibrium always exists between dimer and
455 monomer [36], and for which pI of 6.2 was reported in medaka fish (*Oryzias latipes*) [35] (see
456 Electronic Supplementary Material, Table ESM.2). MDH, cytosolic isoform, is also a
457 homodimer, and in teleost fish the reported mass of its subunit was ~36 kDa [37], and a pI ~7.0
458 [38] (see Electronic Supplementary Material, Table ESM.2). Neither of these two enzymes is
459 an Fe-containing protein, as will be demonstrated bellow. However, the cytosolic fraction
460 isolated in our study from the northern pike liver could additionally contain the proteins that do
461 not bind metals, as well as proteins that bind some other metals, both those that we measured
462 and those that we did not. Moreover, as mentioned earlier, we have found traces of Mn, Pb and
463 Se in the analyzed fraction (see Electronic Supplementary Material, Table ESM.1, Fig. 3),
464 revealing the possibility that our sample contained, in addition to Fe-binding biomolecules, the
465 compounds that contain one of these three elements. The score for FAH was rather low (28-43),
466 the species of its origin was very distant from the studied one (domestic cattle, *Bos taurus*)
467 (Table 5), and the possible cofactors of this enzyme include Mg^{2+} and/or Ca^{2+} [39,40], but we
468 cannot exclude the possibility that our sample contained this enzyme or its monomer. On the
469 other hand, malate dehydrogenase had considerably higher score (97), the species of origin was
470 the same as the studied one (the northern pike) (Table 5), and the known cofactor of this
471 enzyme is Mn^{2+} [41]. Detection of Mn in our sample (Fig. 3a), as well as a small, but clearly

472 visible m/z MALDI-peak at approximately ~36 kDa (Fig. 5b), lead to a conclusion that our
473 studied fraction, in all likelihood, contained, in addition to Fe-binding Hb, Mn-containing
474 malate dehydrogenase or its subunit.

475

476 **4. Conclusions**

477 The analytical approach applied in this study, namely two-dimensional chromatographic
478 separation, enables determination of relationship among various metalloproteins according to
479 their molecular masses and net charges. Furthermore, it is also useful in partial purification of
480 particular metalloproteins, in this case Fe-binding proteins, thus allowing more reliable
481 identification with mass spectrometry techniques. Accordingly, the combination of
482 chromatographic separation and mass spectrometry analysis in this study of Fe-binding
483 biomolecules in the northern pike liver revealed ferritin and Hb as two main participants in Fe-
484 metabolism in this organ, the latter one being the sign of hepatic blood perfusion. Apparent
485 molecular masses of two proteins, estimated by SEC-HPLC, were ~360 kDa and ~50 kDa,
486 respectively, with ferritin having more acidic pI values than Hb, according to AEX-
487 chromatographic separation. The presence of ferritin in the hepatic samples was further
488 demonstrated by detection of probable ferritin subunit at 20.65 kDa by MALDI-TOF-MS. The
489 presence of Hb in the hepatic samples was, on the other hand, confirmed by two techniques of
490 mass spectrometry. MALDI-TOF-MS detected typical m/z spectra with the predominant peak
491 referring to single-charged Hb-monomer (16.1 kDa). LC-MS/MS with subsequent MASCOT
492 database search recognized Hb- β subunits of the northern pike and the sockeye salmon, thus
493 pointing to connection between esocid and salmonid fishes. Further recognition of Mn-binding
494 malate dehydrogenase in our samples revealed that additional separation methods could be
495 applied to obtain better degree of protein purification.

496

497 **Conflicts of interest**

498 There are no conflicts to declare.

499

500 **Author contribution statement**

501 *Zrinka Dragun*: Conceptualization; Data curation; Funding acquisition; Investigation;
502 Methodology; Project administration; Supervision; Validation; Visualization; Roles/Writing -
503 original draft; Writing - review & editing. *Zoran Kiralj*: Formal analysis; Investigation;
504 Methodology; Validation; Resources, Roles/Writing - original draft; Writing - review &
505 editing. *Dušica Ivanković*: Funding acquisition; Investigation; Methodology; Supervision;
506 Writing - review & editing. *Branka Bilić*: Formal analysis; Investigation; Methodology;
507 Validation; Writing - review & editing. *Saša Kazazić*: Investigation; Methodology; Validation;
508 Supervision; Writing - review & editing. *Snježana Kazazić*: Formal analysis; Investigation;
509 Methodology; Validation; Supervision; Roles/Writing - original draft; Writing - review &
510 editing.

511

512 **Ethical approval, Source of biological material, and Statement on animal welfare**

513 Fish were sampled by electrofishing according to the standard CEN EN 14011:2003 and
514 anesthetized and sacrificed according to the Ordinance on the protection of animals used for
515 scientific purposes. Laboratory for Biological Effects of Metals is a laboratory for fish sacrifice
516 and work with fish bodies, organs and tissues, authorized by the Ministry of Agriculture,
517 Veterinary and Food Safety Department (license number: HR-POK-025).

518

519 **Funding**

520 This work has been funded by Croatian Science Foundation under the project “*Metal-binding*
521 *biomolecules and health disturbances of freshwater organisms exposed to industrial wastes*”
522 (METABIOM; IP-2019-04-2636). The financial support of the Ministry of Science and
523 Education of the Republic of Croatia for institutional funding of the Laboratory for Biological
524 Effects of Metals is also acknowledged.

525

526 **Acknowledgements**

527 Special thanks are due to dr. Damir Valić and dr. Tomislav Kralj for fish sampling, to Sara Drk,
528 MSc., for determination of fish age, and to dr. Damir Valić and prof. dr. Jasna Lajtner for
529 consultation regarding fish classification and nomenclature.
530
531

532 **References**

- 533 [1] Muckenthaler MU, Lill R. Cellular iron physiology. In: Anderson GJ, McLaren GD, editors.
534 Iron physiology and pathophysiology in humans. New York: Humana Press; 2012. pp. 27–
535 50.
- 536 [2] Zhao L, Xia Z, Wang F. Zebrafish in the sea of mineral (iron, zinc, and copper) metabolism.
537 Front Pharmacol. 2014;5:33.
- 538 [3] Ding Z, Zhao X, Zhan Q, Cui L, Sun Q, Wang W, Liu H. Comparative analysis of two
539 ferritin subunits from blunt snout bream (*Megalobrama amblycephala*): Characterization,
540 expression, iron depriving and bacteriostatic activity. Fish Shellfish Immunol. 2017;66:411-
541 22.
- 542 [4] Stohs SJ, Bagchi D. Oxidative mechanisms in the toxicity of metal ions. Free Radic Biol
543 Med. 1995;18:321–36.
- 544 [5] Elvitigala DA, Premachandra HK, Whang I, Oh MJ, Jung SJ, Park CJ, Lee J. A teleostean
545 counterpart of ferritin M subunit from rock bream (*Oplegnathus fasciatus*): an active
546 constituent in iron chelation and DNA protection against oxidative damage, with a
547 modulated expression upon pathogen stress. Fish Shellfish Immunol. 2013;35:1455–65.
- 548 [6] Geetha C, Deshpande V. Purification and characterization of fish liver ferritins. Comp
549 Biochem Physiol B. 1999;123:285–94.
- 550 [7] Huang H-Q, Xiao Z-Q, Chen X, Lin Q-M, Cai Z-W, Chen P. Characteristics of structure,
551 composition, mass spectra, and iron release from the ferritin of shark liver (*Sphyrna*
552 *zygaena*). Biophys Chem. 2004;111:213–22.
- 553 [8] Bai L, Xie T, Hu Q, Deng C, Zheng R, Chen W. Genome-wide comparison of ferritin
554 family from archaea, bacteria, eukarya, and viruses: its distribution, characteristic motif,
555 and phylogenetic relationship. Sci Nat. 2015;102:64.

- 556 [9] Lawson DM, Artymiuk PJ, Yewdall SJ, Smith JMA, Livingstone JC, Treffry A, Luzzago
557 A, Levi S, Arosio P, Cesareni G, Thomas CD, Shaw WV, Harrison PM. Solving the
558 structure of human H ferritin by genetically engineering intermolecular crystal contacts.
559 Nature. 1991;349:541–4.
- 560 [10] Zhang S, Guo X, Deng X, Zhao Y, Zhu X, Zhang J. Modifications of thermal-induced
561 northern pike (*Esox lucius*) liver ferritin on structural and self-assembly properties. Foods.
562 2022;11:2987.
- 563 [11] Perutz MF. Hemoglobin structure and respiratory transport. Sci Am. 1978; 239:92–125.
- 564 [12] Giardina B, Mosca D, De Rosa MC. The Bohr effect of haemoglobin in vertebrates: an
565 example of molecular adaptation to different physiological requirements. Acta Physiol
566 Scand. 2004;182:229–44.
- 567 [13] de Souza PC, Bonilla-Rodriguez GO. Fish hemoglobins. Braz. J Med Biol Res.
568 2007;40:769–78.
- 569 [14] Krasnići N, Dragun Z, Kazazić S., Muharemović H, Erk M, Jordanova M, Rebok K,
570 Kostov V. Characterization and identification of selected metal-binding biomolecules from
571 hepatic and gill cytosols of Vardar chub (*Squalius vardarensis* Karaman, 1928) using
572 various techniques of liquid chromatography and mass spectrometry. Metallomics.
573 2019;11:1060–78.
- 574 [15] Krasnići N, Dragun Z, Erk M, Raspor B. Distribution of selected essential (Co, Cu, Fe,
575 Mn, Mo, Se and Zn) and nonessential (Cd, Pb) trace elements among protein fractions from
576 hepatic cytosol of European chub (*Squalius cephalus* L.). Environ Sci Pollut Res.
577 2013;20:2340–51.
- 578 [16] Dragun Z, Krasnići N, Kolar N, Filipović Marijić V, Ivanković D, Erk M. Cytosolic
579 distributions of highly toxic metals Cd and Tl and several essential elements in the liver of

580 brown trout (*Salmo trutta* L.) analyzed by size exclusion chromatography and inductively
581 coupled plasma mass spectrometry. *Chemosphere*. 2018;207:162–73.

582 [17] Dragun Z, Krasnići N, Ivanković D, Filipović Marijić V, Mijošek T, Redžović Z, Erk M.
583 Comparison of intracellular trace element distributions in the liver and gills of the invasive
584 freshwater fish species, Prussian carp (*Carassius gibelio* Bloch, 1782). *Sci Total Environ*.
585 2020;730:138923.

586 [18] Dragun Z, Ivanković D, Krasnići N, Kiralj Z, Cvitanović M, Karamatić I, Valić D, Barac
587 F, Filipović Marijić V, Mijošek T, Gjurčević E, Matanović K, Kužir S. Metal-binding
588 biomolecules in the liver of northern pike (*Esox lucius* Linnaeus, 1758): The first data for
589 the family Esocidae. *Comp Biochem Physiol C*. 2022;257:109327.

590 [19] Dragun Z, Kiralj Z, Pećnjak A, Ivanković D. The study of acidic/basic nature of
591 metallothioneins and other metal-binding biomolecules in the soluble hepatic fraction of the
592 northern pike (*Esox lucius*). *Int J Biol Macromol*. 2024;256:128209.

593 [20] HRN EN 14011. Fish Sampling by Electric Power [Uzorkovanje riba električnom
594 strujom]. 2005.

595 [21] NN 55. Ordinance on the Protection of Animals Used for the Scientific Purposes
596 [Pravilnik o zaštiti životinja koje se koriste u znanstvene svrhe]. 2013.

597 [22] Bonneris E, Giguère A, Perceval O, Buronfosse T, Masson S, Hare L, Campbell PGC.
598 Sub-cellular partitioning of metals (Cd, Cu, Zn) in the gills of a freshwater bivalve,
599 *Pyganodon grandis*: role of calcium concretions in metal sequestration. *Aquat Toxicol*.
600 2005;71:319–34.

601 [23] de la Calle Guntiñas MB, Bordin G, Rodriguez AR. Identification, characterization and
602 determination of metal-binding proteins by liquid chromatography. A review. *Anal Bioanal*
603 *Chem*. 2002;374:369–78.

- 604 [24] Rodríguez-Cea A, Linde Arias AR, Fernández de la Campa MR, Costa Moreira J, Sanz-
605 Medel A. Metal speciation of metallothionein in white sea catfish, *Netuma barba*, and pearl
606 cichlid, *Geophagus brasiliensis*, by orthogonal liquid chromatography coupled to ICP-MS
607 detection. *Talanta*. 2006;69:963–9.
- 608 [25] Krasnići N, Dragun Z, Erk M, Ramani S, Jordanova M, Rebok K, Kostov V. Size-
609 exclusion HPLC analysis of trace element distributions in hepatic and gill cytosol of Vardar
610 chub (*Squalius vardarensis* Karaman) from mining impacted rivers in North-Eastern
611 Macedonia. *Sci Total Environ*. 2018;613–614:1055–68.
- 612 [26] Falk TM, Villwock W, Renwranz L. Heterogeneity and subunit composition of the
613 haemoglobins of five tilapiine species (Teleostei, Cichlidae) of the genera *Oreochromis* and
614 *Sarotherodon*. *J Comp Physiol B*. 1998;168:9–16.
- 615 [27] Aisen P, Enns C, Wessling-Resnick M. Chemistry and biology of eukaryotic iron
616 metabolism. *Int J Biochem Cell Biol*. 2001;33:940–59.
- 617 [28] Beard JL, Dawson H, Pifiero DJ. Iron metabolism: a comprehensive review. *Nutr Rev*.
618 1996;54:295–317.
- 619 [29] Qiao J., Du Z, Zhang Y, Du H, Guo L, Zhong M, Cao J, Wang X. Proteomic identification
620 of the related immune-enhancing proteins in shrimp *Litopenaeus vannamei* stimulated with
621 vitamin C and Chinese herbs. *Fish Shellfish Immunol*. 2011;31:736–45.
- 622 [30] Okai CA, Wölter M, Russ M, Koy C, Petre BA, Rath W, Pecks U, Glocker MO. Profiling
623 of intact blood proteins by matrix-assisted laser desorption/ionization mass spectrometry
624 without the need for freezing – Dried serum spots as future clinical tools for patient
625 screening. *Rapid Commun Mass Spectrom*. 2021;35:e9121.
- 626 [31] Almeida-Val VMF, Val AL. Adaptação bioquímica em peixes da Amazônia. *Cienc Hoje*.
627 1992;120:124–9.

- 628 [32] Habara Y, Urushiyama S, Shibuya T, Ohshima Y, Tani T. Mutation in the *prp12⁺* gene
629 encoding a homolog of SAP130/SF3b130 causes differential inhibition of pre-mRNA
630 splicing and arrest of cell-cycle progression in *Schizosaccharomyces pombe*. RNA.
631 2001;7:671–81.
- 632 [33] Barik S. Suppression of innate immunity by the hepatitis C virus (HCV): Revisiting the
633 specificity of host–virus interactive pathways. Int J Mol Sci. 2023;24:16100.
- 634 [34] Della Torre C, Zaja R, Loncar J, Smital T, Focardi S, Corsi I. Interaction of ABC transport
635 proteins with toxic metals at the level of gene and transport activity in the PLHC-1 fish cell
636 line. Chem Biol Interact. 2012;198:9–17.
- 637 [35] Malécot M, Mezhoud K, Marie A, Praseuth D, Puiseux-Dao S, Edery M. Proteomic study
638 of the effects of microcystin-LR on organelle and membrane proteins in medaka fish liver.
639 Aquat Toxicol. 2009;94:153–61.
- 640 [36] Macias I, Laín A, Bernardo-Seisdedos G, Gil D, Gonzalez E, Falcon-Perez JM, Millet O.
641 Hereditary tyrosinemia type I–associated mutations in fumarylacetoacetate hydrolase
642 reduce the enzyme stability and increase its aggregation rate. J Biol Chem.
643 2019;294:13051–60.
- 644 [37] Lin J-J, Yang T-H, Wahlstrand BD, Fields PA, Somero GN. Phylogenetic relationships
645 and biochemical properties of the duplicated cytosolic and mitochondrial isoforms of
646 malate dehydrogenase from a teleost fish, *Sphyaena idiaestes*. J Mol Evol. 2002;54:107–17.
- 647 [38] Merrit TJS, Quattro JM. Evolution of the vertebrate cytosolic malate dehydrogenase gene
648 family: duplication and divergence in actinopterygian fish. J Mol Evol. 2003;56:265–76.
- 649 [39] Timm DE, Mueller HA, Bhanumoorthy P, Harp JM, Bunick GJ. Crystal structure and
650 mechanism of a carbon–carbon bond hydrolase. Structure. 1999;7:1023–33.

651 [40] Bateman RL, Bhanumoorthy P, Witte JF, McClard RW, Grompe M, Timm DE.
652 Mechanistic inferences from the crystal structure of fumarylacetoacetate hydrolase with a
653 bound phosphorus-based inhibitor. J Biol Chem. 2001;276:15284–91.

654 [41] Milne JA, Cook RA. Role of metal cofactors in enzyme regulation. Differences in the
655 regulatory properties of the *Escherichia coli* nicotinamide adenine dinucleotide specific
656 malic enzyme depending on whether Mg²⁺ or Mn²⁺ serves as divalent cation. Biochemistry.
657 1981;20:2503–12.

658

659 **Figure captions**

660 **Figure 1.** The Fe distribution profiles established by online coupled HPLC-ICP-MS with
661 anion-exchange (AEX) column for the hepatic cytosols of the three northern pike specimens
662 (samples 1-3), caught in the Mrežnica River (Croatia) in front of the former cotton industry
663 facility in Duga Resa town in April/May 2021. The results are presented as Fe intensities (y-
664 axis) versus elution time (E_t , min; x-axis). The maxima for two major Fe-AEX-peaks of each
665 sample are annotated within the figure, as well as the cytosolic Fe concentrations.

666 **Figure 2.** The Fe distribution profiles established by online coupled HPLC-ICP-MS with size-
667 exclusion (SEC_{200}) column in the four selected chromatographic fractions obtained by AEX-
668 HPLC separation of the hepatic cytosols of the two northern pike specimens (samples 1-2),
669 caught in the Mrežnica River (Croatia) in front of the former cotton industry facility in Duga
670 Resa town in April/May 2021: a) AEX-fraction A: 8.5-9.5 min; b) AEX-fraction B: 9.5-10.0
671 min; c) AEX-fraction C: 10.0-10.5 min; d) AEX-fraction D: 10.5-11.5 min. The results are
672 presented as in the Fig. 1. The maxima (E_t , min; and estimated molecular masses according to
673 SEC-column calibration, kDa) for the major Fe-SEC-peaks of each sample are annotated within
674 the figures for each AEX-fraction.

675 **Figure 3.** The distribution profiles established by online coupled HPLC-ICP-MS with size-
676 exclusion (SEC_{200}) column for additional three metals in a single chromatographic fraction
677 obtained by AEX-HPLC separation of the hepatic cytosols of the two northern pike specimens
678 (samples 1-2), caught in the Mrežnica River (Croatia) in front of the former cotton industry
679 facility in Duga Resa town in April/May 2021 (namely, AEX-fraction B; 9.5-10.0 min): a) Mn;
680 b) Pb; and c) Se. The results are presented as in the Fig. 2.

681 **Figure 4.** The distribution profiles established by online coupled HPLC-ICP-MS with size-
682 exclusion (SEC_{200}) column for additional two metals in a single chromatographic fraction
683 obtained by AEX-HPLC separation of the hepatic cytosols of the two northern pike specimens
684 (samples 1-2), caught in the Mrežnica River (Croatia) in front of the former cotton industry
685 facility in Duga Resa town in April/May 2021 (namely, AEX-fraction C; 10.0-10.5 min): a) Pb;
686 and b) Zn. The results are presented as in the Fig. 2.

687 **Figure 5.** Mass spectra obtained by MALDI-TOF-MS for fish sample 2: a) ~360 kDa Fe-
688 binding biomolecule isolated by two-dimensional chromatographic separation (AEX-HPLC
689 (fraction C, 10.0-10.5 min) followed by SEC-HPLC (peak 1, 17-19 min)); b) ~50 kDa Fe-
690 binding biomolecule isolated by two-dimensional chromatographic separation (AEX-HPLC
691 (fraction B, 9.5-10.0 min) followed by SEC-HPLC (peak 2, 23-26 min)). The results are
692 presented as intensities (y-axis) versus m/z values (x-axis). The maxima of decisive peaks are
693 annotated within the figure (m/z).

Northern pike (*Esox lucius*)



Liver

**Study of Fe
in the liver of
the northern pike**

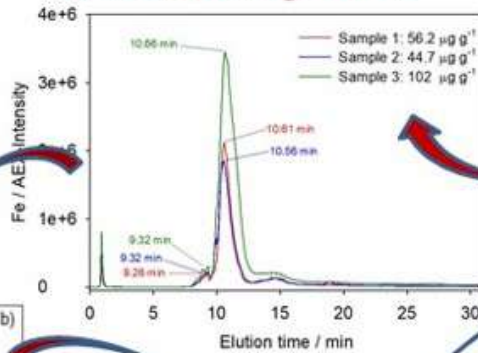
Liver dissection

homogenization

centrifugation (at 50,000xg)

cytosol (supernatant, S50)

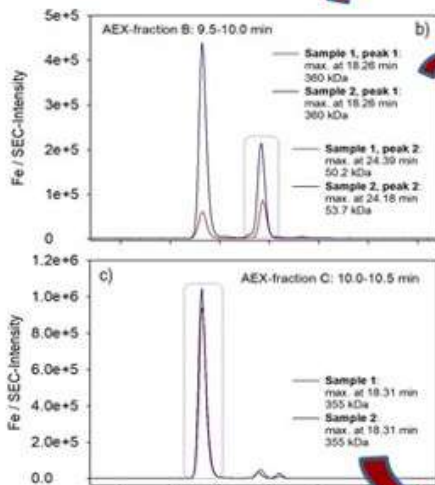
Anion-exchange HPLC



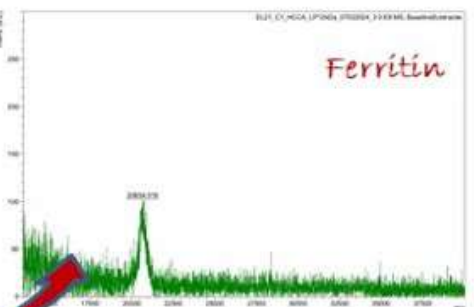
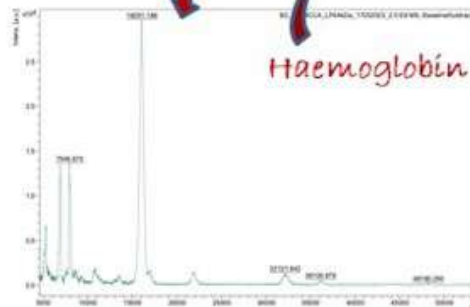
LC-MS/MS + Mascot search:

- haemoglobin subunit β
- *Esox lucius*
- *Oncorhynchus nerka*

Size-exclusion HPLC



MALDI-TOF-MS



- two-dimensional chromatographic separation proven useful for protein purification
- ferritin and Hb, main Fe-metalloproteins in soluble northern pike liver fraction
- MALDI-TOF-MS m/z peaks at 20.65 and 16.05 kDa indicated ferritin and Hb subunits
- LC-MS/MS analysis with MASCOT database search recognized Hb- β subunits
- MASCOT database search revealed similarity between esocid and salmonid fishes

Figure 1.

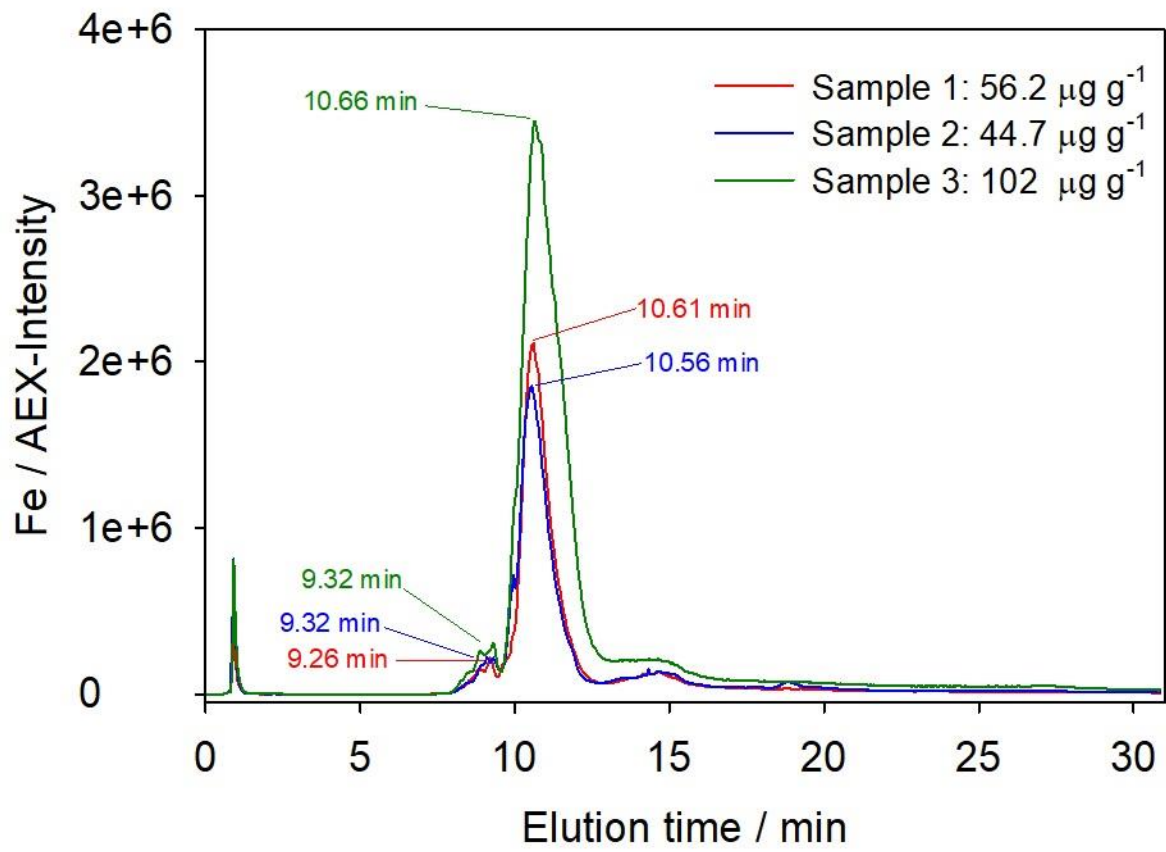


Figure 2.

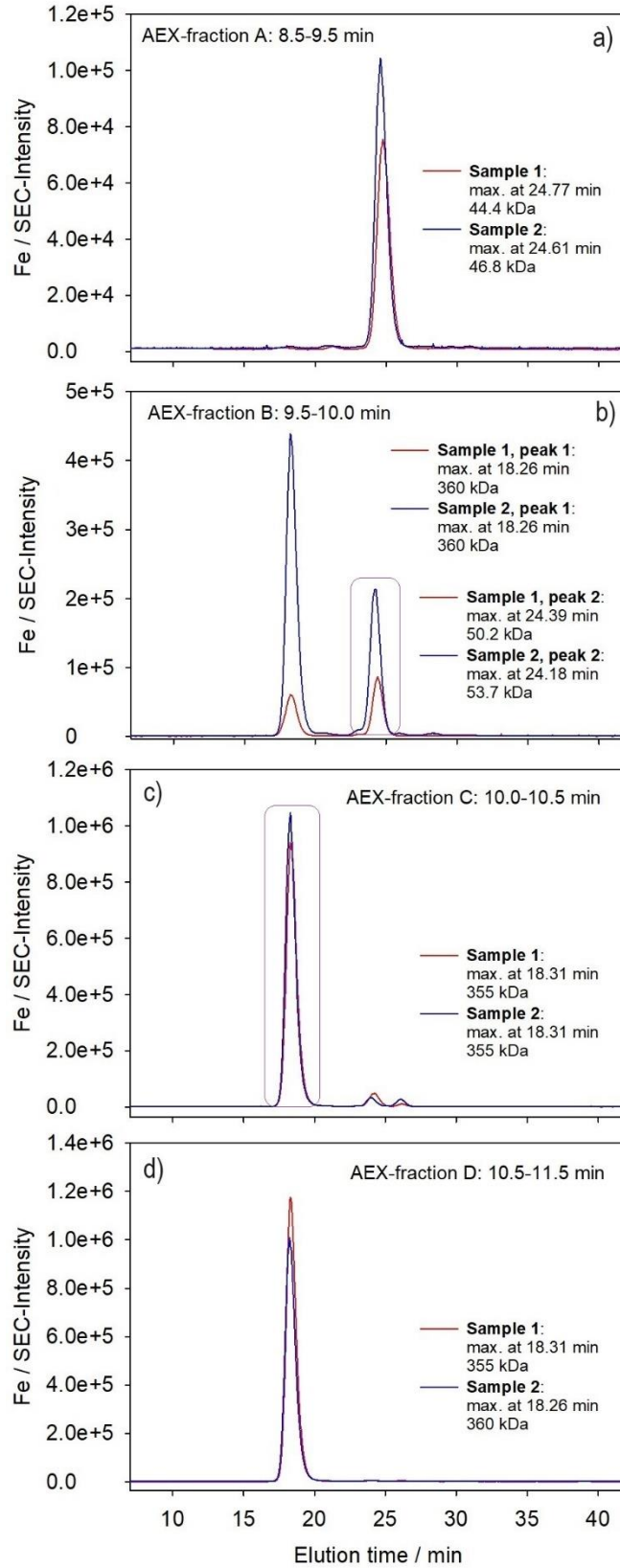


Figure 3.

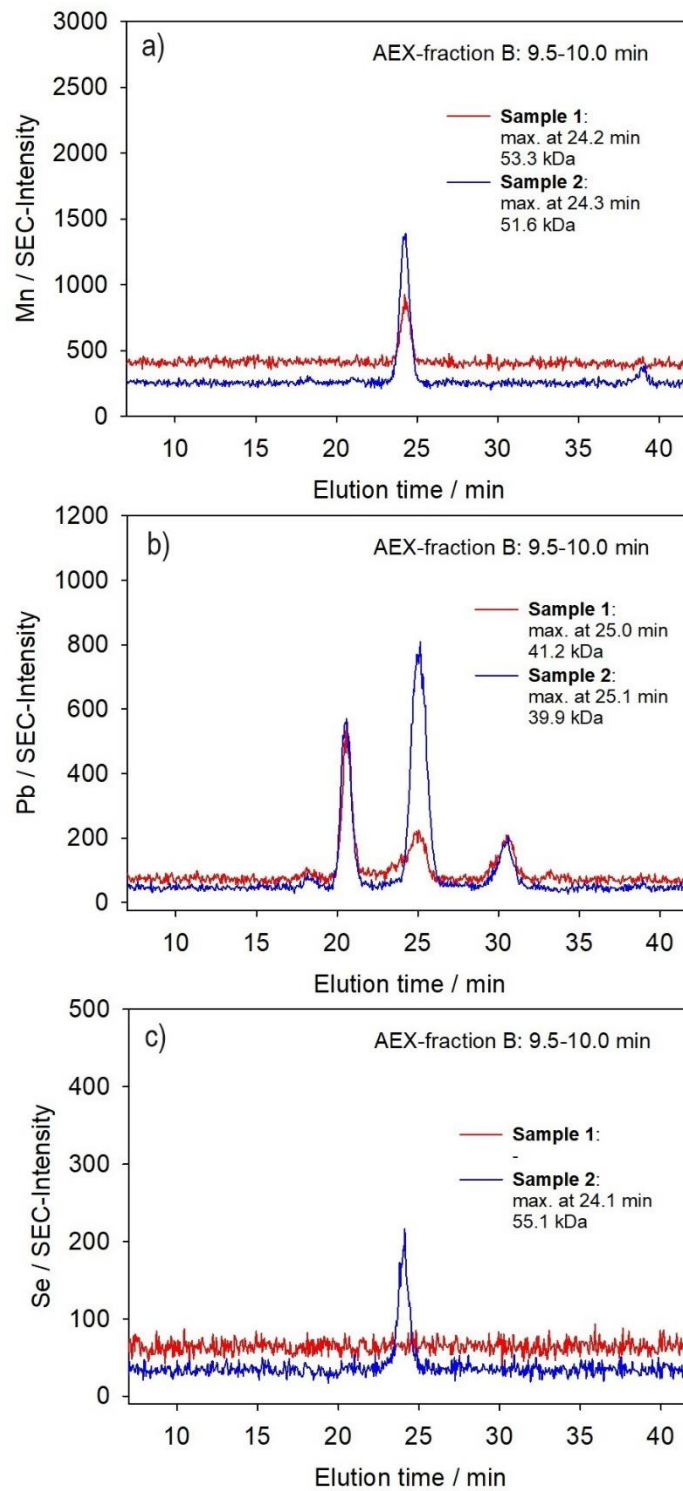


Figure 4.

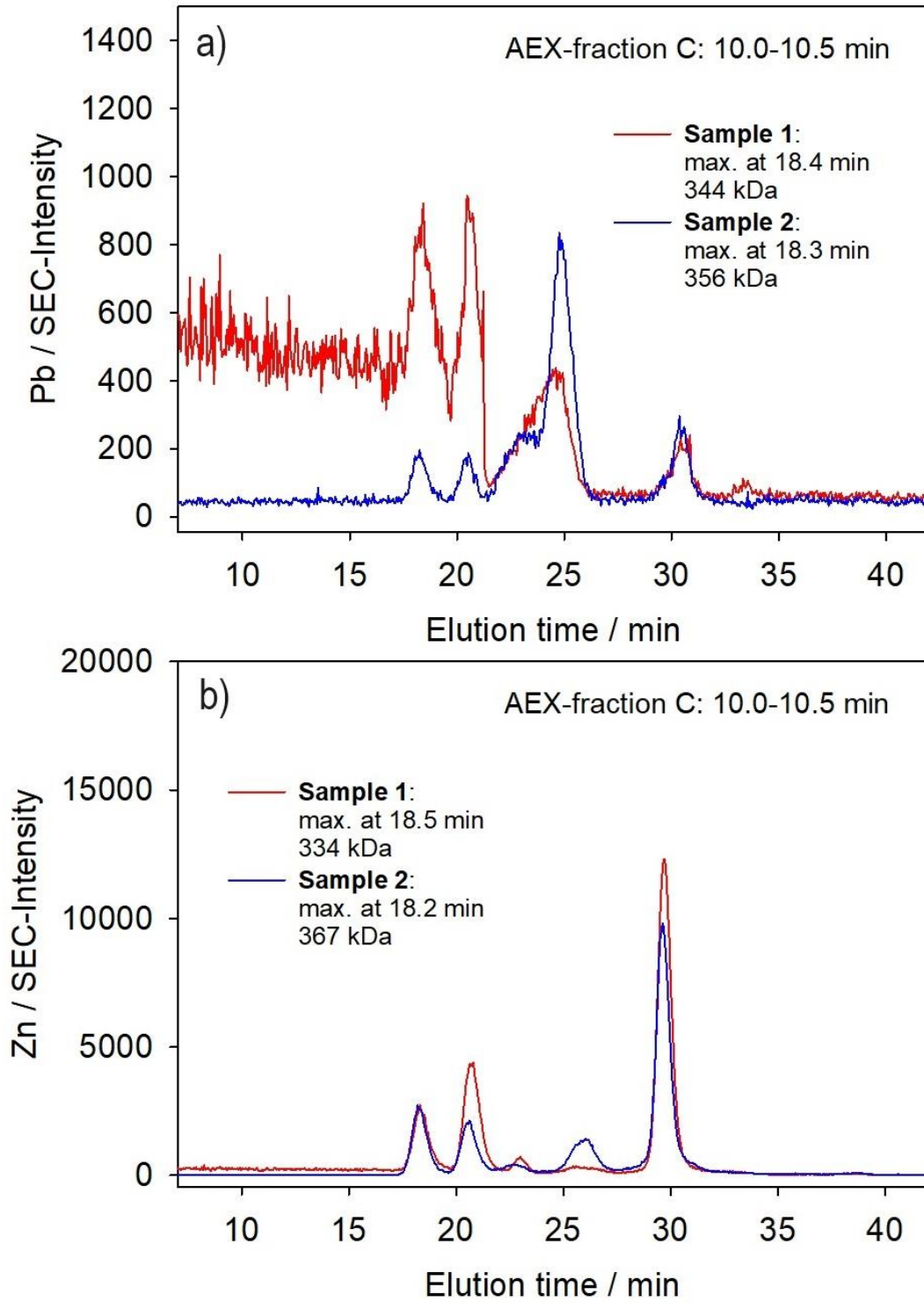


Figure 5.

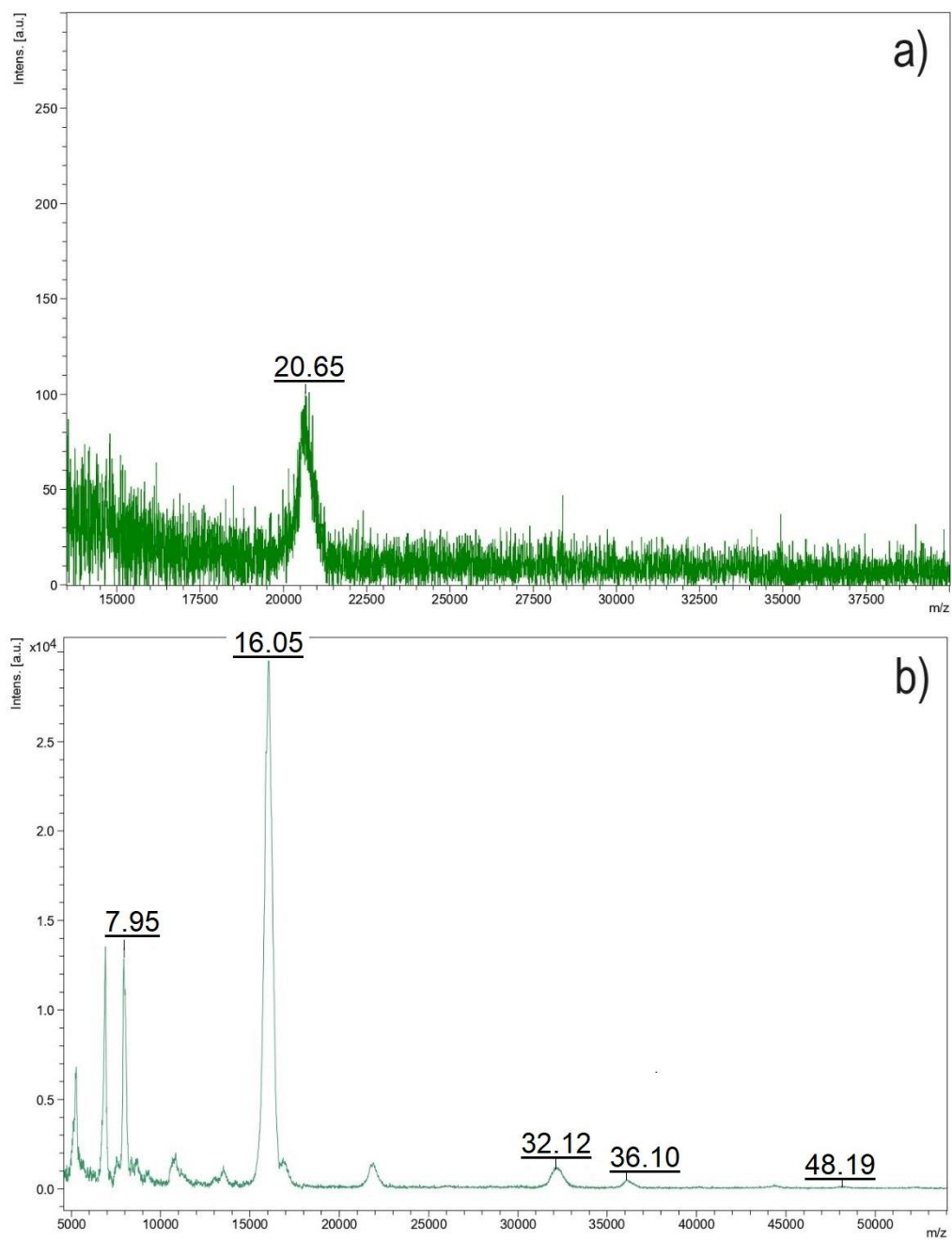


Table 1. The cytosolic concentrations of Fe and 13 other trace elements in the liver of the three specimens of the northern pike used in this study, and caught from the Mrežnica River (Croatia) in front of the former cotton industry facility in Duga Resa town in April/May 2021.

	Sample 1	Sample 2	Sample 3
Ag / ng g⁻¹	14.2	20.1	17.0
As / ng g⁻¹	17.3	16.7	16.6
Bi / ng g⁻¹	8.73	7.07	12.7
Cd / ng g⁻¹	5.12	0.68	19.8
Co / ng g⁻¹	12.7	14.5	16.3
Cs / ng g⁻¹	3.65	4.72	5.44
Cu / μg g⁻¹	3.64	3.99	4.85
Fe / μg g⁻¹	56.2	44.7	102
Mn / ng g⁻¹	519	419	433
Mo / ng g⁻¹	52.6	67.4	55.0
Pb / ng g⁻¹	<LOD*	<LOD	<LOD
Se / ng g⁻¹	271	641	585
Tl / ng g⁻¹	4.70	6.32	5.47
Zn / μg g⁻¹	19.8	22.7	21.1

* LOD for Pb: 0.49 ng g⁻¹

Table 2. Separation protocols for analysing Fe-binding biomolecules from the soluble hepatic fraction of the northern pike by anion-exchange (AEX) and size-exclusion (SEC) HPLC.

	AEX-HPLC	SEC-HPLC
Column	MonoQ™ 5/50 GL (GE Healthcare BioSciences, USA)	Superdex® 200 Increase 10/300 GL (Cytiva, USA) separation range of 10–600 kDa
Dimensions	5×50 mm	10×300 mm
Mobile phase	<u>A</u> : 4 mM Tris-HCl/Base (Sigma Aldrich, USA; pH 7.4, 22 °C) <u>B</u> : 10 mM Tris-HCl/Base (Sigma Aldrich, USA) + 500 mM ammonium acetate (NH ₄ OAc; Merck KgaA, Germany) (pH 7.4, 22 °C)	<u>A</u> : 20 mM Tris-HCl/Base (Sigma Aldrich, USA; pH 8.1, 22 °C)
Sample injection volume	100 µL	100 µL
Flow rate	1.0 mL min ⁻¹	0.5 mL min ⁻¹
Method	1 st step: mobile phase A 100%, 5 min 2 nd step: linear gradient 0-100% mobile phase B, 20 min 3 rd step: mobile phase B 100%, 5 min	1 st step: mobile phase A 100%, 60 min

Table 3. Concentrations, sources, elution times (t_e) and molecular masses (MM) of blue dextran (for determination of void volume) and six standard proteins used for calibration of Superdex® 200 Increase 10/300 GL (Cytiva) size exclusion column. Equation of calibration straight line was: $y = -0.2256x + 1.3165$; ($y = K_{av}$; $x = \log MM$).

Protein standard	Source	Concentration / mg mL⁻¹	t_e / min	MM / kDa
Blue dextran	<i>Leuconostoc mesenteroides</i>	1	16.26	2000
Thyroglobulin	Bovine thyroid	5	16.79	669
Apoferritin	Equine spleen	3	17.84	443
β -amylase	Sweet potato	4	19.49	200
Alcohol dehydrogenase	<i>Saccharomyces cerevisiae</i>	5	20.65	150
Transferrin	Human	1	22.57	80
Superoxide dismutase	Bovine erythrocytes	5	26.38	32

Table 4. The main hits obtained by the LC-MS/MS analyses with MASCOT search of two databases for the following chromatographically separated and collected fraction: AEX-HPLC fraction B (9.5-10.0 min; Figs. 1-2) further fractionated by SEC-column (peak 2; 23-26 min; HPLC-estimated molecular mass of intact protein (MM): ~30-80 kDa; Fig. 2b). The presented results refer to obtained hits for Fe-containing proteins of adequate molecular masses, with the highest scores and overlapping in both databases. The complete MASCOT search results are presented as Supplementary Information.

	Database	Compound	Species	MM / Da	Score	Matches	Sequences	emPAI
Sample 1	UniProt/Swiss-Prot	Haemoglobin subunit β	<i>Oncorhynchus nerka</i>	16214	66	6(1)	3(1)	0.2
	NCBIInr	Haemoglobin subunit β	<i>Esox lucius</i>	16574	145	4(0)	4(0)	0.2
Sample 2	UniProt/Swiss-Prot	Haemoglobin subunit β	<i>Oncorhynchus nerka</i>	16214	45	5(0)	2(0)	0.2
	NCBIInr	Haemoglobin subunit β -like	<i>Esox lucius</i>	16405	38	3(1)	2(1)	0.2

Table 5. The additional hits obtained by the LC-MS/MS analyses with MASCOT search of two databases for the following chromatographically separated and collected fraction: AEX-HPLC fraction B (9.5-10.0 min; Figs. 1-2) further fractionated by SEC-column (peak 2; 23-26 min; HPLC-estimated molecular mass of intact protein (MM): ~30-80 kDa; Fig. 2b). The complete MASCOT search results are presented as Supplementary Information.

	Database	Compound	Species	MM / kDa	Score
Sample 1	UniProt/Swiss-Prot	Ribosomal RNA large subunit methyl-transferase	<i>Rhodopseudomonas palustris</i>	17.94	45
		Fumaryl-acetoacetase	<i>Bos taurus</i>	46.53	28
		DNA-directed RNA polymerase subunit β	<i>Rickettsia africae</i>	154.8	26
		DNA-directed RNA polymerase subunit β	<i>Rickettsia canadensis</i>	154.5	26
		Caskin-2	<i>Xenopus laevis</i>	131.6	23
	NCBIInr	Malate dehydrogenase, cytoplasmic isoform X1	<i>Esox lucius</i>	38.37	97
Sample 2	UniProt/Swiss-Prot	Fumaryl-acetoacetase	<i>Bos taurus</i>	46.53	43
		Pre-mRNA-splicing factor prp12	<i>Schizosaccharomyces pombe</i>	135.8	32
		Genome polyprotein	<i>Hepatitis C virus</i>	333.1	27
		30S ribosomal protein S3	<i>Methylobacillus flagellatus</i>	26.32	27
	NCBIInr	tRNA (Met) cytidine acetyltransferase	<i>Mucor circinelloides</i>	120.7	45
		ATP-binding cassette domain-containing protein	<i>Halospina sp.</i>	40.42	37